High-β steady-state scenarios in DIII-D with on-axis current drive

C.C. Petty[1], J.R. Ferron[1], F. Turco[2], J.M. Park[3], A.M. Garofalo[1], A.W. Hyatt[1], G.L. Jackson[1], T.C. Luce[1], C.T. Holcomb[4], E.J. Doyle[5] and W.M. Solomon[6]

[1]*General Atomics, P.O. Box 85608, San Diego, CA 92186-5608, USA*
[2]*Columbia University, 116th St and Broadway, New York, NY 10027, USA*
[3]*Oak Ridge National Laboratory, P.O. Box 2008, Oak Ridge, TN 37831, USA*
[4]*Lawrence Livermore National Laboratory, 700 East Ave, Livermore, CA 94550, USA*
[5]*University of California Los Angeles, Los Angeles, CA* 90095-7099, *USA*
[6]*Princeton Plasma Physics Laboratory, Princeton, NJ*, *USA*

Abstract. Experiments in the DIII-D tokamak have demonstrated potential new paths to fusion steady state based on peaked current profiles with $q_{min}\approx1$ that have high ideal stability limits, excellent confinement and benefit from efficient on-axis current drive. In the hybrid scenario, steady-state conditions (V_{surf}=0) using central ECCD and NBCD are achieved in 1.0 MA discharges with a beta value (β_N=3.6) that is 80%-90% of the ideal n=1 with-wall limit. Interestingly, the hybrid mechanism that anomalously broadens the current profile to maintain $q_{min}>1$ and prevents sawteeth continues to function despite the intense central current drive. In the "high ℓ_i" scenario, the combination of broad pressure profile and a peaked current profile tailored to maximize ℓ_i allows $\beta_N\approx4.8$ and $H_{98y2}\approx1.8$ to be achieved transiently in a discharge that is overdriven ($V_{surf}<0$). The achieved β_N is near the no-wall limit with the ideal-wall limit higher at $\beta_N\approx5$-6.

I. Introduction

This paper discusses two high-β scenarios in DIII-D with on-axis current drive that are consistent with the Q=5 steady-state mission in ITER. While both cases have $q_{min}\approx1$, the hybrid scenario relies on the self-organized current profile produced by that regime, whereas the high ℓ_i scenario takes a more active approach to create an optimized current profile. Hybrid plasmas have the advantage of robustness and insensitivity to the current drive profile; the high ℓ_i scenario is more complex but has higher stability limits and higher confinement, as well as a less critical need for a high pedestal.

II. Steady-State Hybrid Scenario

In DIII-D, experiments show that the beneficial characteristics of the hybrid scenario are maintained when central co-current drive is applied to increase the non-inductive fraction to ≈100% [1]. The advantages of the hybrid regime over the $q_{min}>2$ Advanced Tokamak (AT) regime are (1) good alignment between the current drive and plasma current profile is not necessary as poloidal magnetic flux pumping self-organizes the current density profile in hybrids with an m/n=3/2 tearing mode [2], and (2) the current drive in hybrids can be located near the plasma center where the current drive efficiency is highest. The high current drive efficiency can fully compensate for a lower bootstrap current fraction in the $q_{min}\approx1$ regime compared to the $q_{min}>2$ AT regime.

The natural attributes of the hybrid scenario make it a robust regime for high-β, steady-state plasmas, as shown in Fig. 1 where the surface loop voltage V_{surf}=0, thermal confinement factor $H_{98(y,2)}$=1.56 and normalized beta β_N=3.64 (toroidal beta β_T=3.1%) are sustained for the maximum duration of the beam pulse without exciting the deleterious m/n=2/1 tearing mode. Half of the plasma current is driven non-inductively near the plasma center by electron cyclotron current drive (ECCD) and neutral beam current drive (NBCD), with the other half

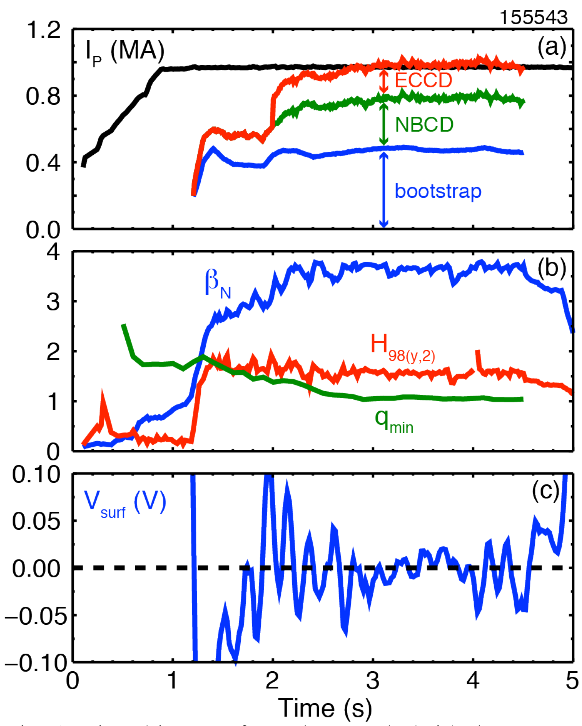

Fig. 1: Time history of steady-state hybrid plasma.

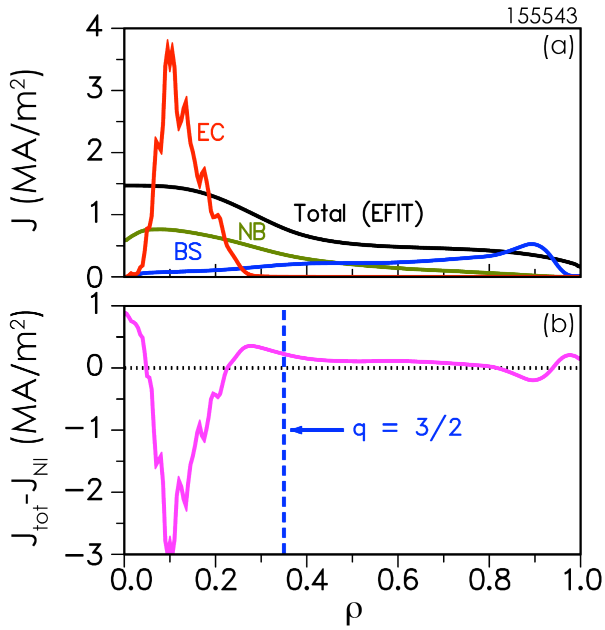

Fig. 2: (a) Total current density from EFIT, and modeled current densities from ECCD, NBCD and bootstrap. (b) Difference between total current density from EFIT and modeled non-inductive current densities.

generated by the bootstrap current. The non-inductive currents calculated by TRANSP are overlaid with the measured plasma current in Fig. 1a. While this demonstrates that V_{surf}=0 is consistent with the calculated non-inductive currents, Fig. 2a shows that the reconstructed current profile is not consistent with the sum of the driven current profiles. The current profile anomaly is displayed in Fig. 2b, where the calculated non-inductive current density is subtracted from the total current density determined by equilibrium reconstruction. Inside of the q=3/2 surface, the current profile is strongly overdriven and the current relaxation time is sufficiently short that q_{min} should drop below 1 by the end of the discharge. The fact that q_{min} remains above unity and sawteeth are absent shows that the hybrid scenario maintains an anomalously broad current profile even in the presence of strong central current drive.

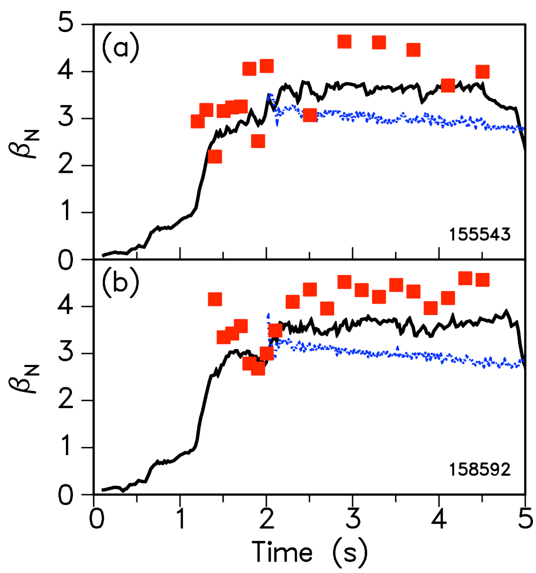

Fig. 3: Comparison of measured β_N (solid black line), ideal-wall (red squares) and no-wall (dotted blue line) n=1 limits for (a) mixed on/off-axis beams and (b) on-axis beams.

The beta value obtained in steady-state hybrids is 80%-90% of the ideal n=1 with-wall limit. The theoretical stability limits are calculated by the DCON code using EFIT reconstructions constrained by the experimental pressure profile, MSE polarimetry and a neoclassical calculation of the pedestal bootstrap current density. These experiments utilized both on-axis and off-axis beam deposition (two of the six co-beams can inject off-axis) to affect the stability limit by varying the pressure profile peakedness (f_P=P_0/<P>). Figure 3 shows that in hybrids with complete current drive, β_N=3.64 (i.e., β_N=4.9ℓ_i) is reached and maintained for the duration of high power NBI. This value exceeds the no-wall n=1 stability limit (average DCON value β_N=4ℓ_i) and is close to the ideal-wall n=1 limit. Using off-axis beam power reduces f_P from ~3.4 to ~3.1, mainly by changing the fast ion pressure profile, with the largest systematic differences between on/off-axis injection occurring for β_N>3.3. On average the DCON calculated ideal-wall limit is ≈10% higher for hybrid plasmas with off-axis beam injection, but experimentally little difference is seen in the maximum beta (β_N=4.0 for 0.8 s) with or without off-axis beam power. Future plans have DIII-D increasing the number of off-axis beams from two to four, and the number of co-beams from six to eight, which may allow the theoretical advantages of a broader pressure profile to be more easily realized.

III. High ℓ_i Scenario

By taking a more active approach in tailoring the peaked current profile to maximize ℓ_i, the ideal stability limit and confinement can be increased beyond the more passive approach described in the previous section. These performance improvements arise largely as a result of higher poloidal field in the discharge core and larger magnetic shear in the outer half of the plasma. The benefits of this "high ℓ_i" scenario are seen in Fig. 4, where β_N≈4.8 and $H_{98(y,2)}$≈1.8 are achieved transiently at ℓ_i≈1.3 [3]. To form the high ℓ_i target, the discharge begins with a long ohmic phase so that the electron temperature is low and the current density profile becomes peaked in the core with q_{min}≈1. Next, ECCD at ρ≈0.4 is added to increase the electron temperature and "freeze in" the peaked current profile, after which high power beam heating is applied to transition the plasma into ELMy H-mode and ramp up β_N. As described later, the ohmic current profile slowly becomes less peaked in time during the H-mode phase, resulting in the decreasing confinement time (and thus decreasing β_N at fixed heating power) seen in Fig. 4 as ℓ_i evolves to a lower value.

Plasmas with high ℓ_i and β_N=4-5 are predicted to be stable to low-n ideal MHD instabilities even without the effect of a conducting wall. As seen in Fig. 5, the peak β_N for the discharge shown in Fig. 4 is near the no-wall n=1 limit calculated by DCON, with the ideal-wall n=1 limit higher at β_N≈5-6. The ideal infinite-n ballooning mode stability limit calculated using the BALOO code is slightly below that of the ideal-wall n=1 mode. Consistent with these stability calculations, a global, pressure-limiting instability has not yet been clearly observed in the experiment. Instead, in cases where stability determines the limit to performance (such as when β_N is raised above 5), the observed mode is most commonly a m/n=2/1 resistive tearing mode.

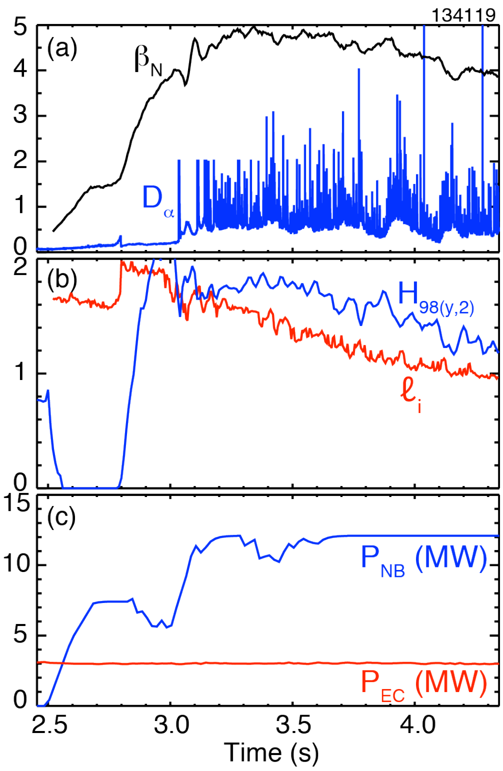

Fig. 4: Time history of high ℓ_i discharge.

Broadening of the pressure profile with increasing β_N plays an important role in enabling stable access to high plasma pressure along with the elevated values of ℓ_i. The broad pressure profiles obtained in these high ℓ_i plasmas, f_P~2.5, strongly increases the ideal-wall stability limit [4]. Interestingly, a low H-mode pedestal height, which can result from pedestal physics and/or the application of 3D magnetic fields, is not necessarily detrimental to this steady-state scenario as it works to raise ℓ_i and thus the ideal-wall limit. As a result, the high ℓ_i scenario is a promising option for the ITER Q=5 steady-state mission that can perform well in plasmas with a low pedestal height.

The elevated ℓ_i in present experiments is largely a result of the inductively-driven current profile. Figure 6 displays the individual current density components (bootstrap, NBCD, ECCD and ohmic),

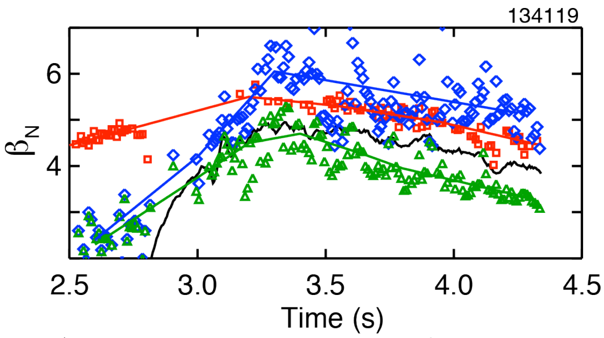

Fig. 5: Comparison of experimental β_N and no-wall (triangles) and ideal-wall (diamonds) n=1 stability limits. The squares are the ideal infinite-n ballooning mode stability limit. The lines are sketches to indicate the location of various sets of data points.

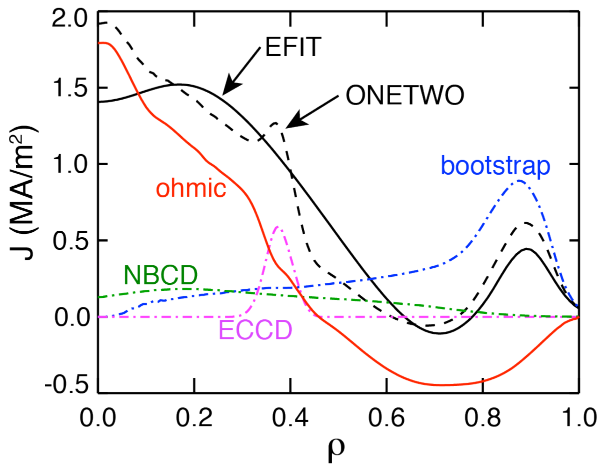

Fig. 6: Total current density profiles obtained from an equilibrium reconstruction and as calculated by ONETWO. The individual current density components from ONETWO are also plotted.

as well as the total current density, calculated by the ONETWO transport code for the discharge in Fig. 4 at 3.35 s; for reference, the total current density profile from a well-constrained equilibrium reconstruction is also plotted. The plasma current is actually overdriven with a bootstrap current fraction of ≈80% and V_{surf}<0. The negative surface loop voltage penetrates relatively quickly through the outer half of the plasma, with the negative inductively-driven current density outside ρ=0.5 offsetting some of the bootstrap current, helping to maintain an elevated value of ℓ_i. The negative loop voltage penetrates slowly towards the axis during the high β_N phase, decreasing the ohmic current in the plasma center and causing ℓ_i to drop over time. With a long enough pulse duration, this discharge would eventually evolve to a relatively low ℓ_i case because of the high pedestal bootstrap current.

To make the high ℓ_i scenario not only fully non-inductive but also stationary, the portion of the evolving ohmic current driven by the positive loop voltage in the core needs to be replaced with on-axis ECCD and NBCD (and higher plasma current is needed to eliminate the negative loop voltage). The maximum value of ℓ_i that can be obtained by tailoring the profile of the externally-driven current density will decrease with increasing bootstrap current in the outer half of the plasma. Therefore, the "optimized high ℓ_i" equilibrium has about 50% bootstrap current and 50% external current drive near the axis. Transport code modeling of the steady-state current profile using TGLF [5] to self-consistently predict the temperature profiles examined the accessible current density and pressure profiles to maximize the stationary value of β_N consistent with the calculated stability limits. The result of this modeling study is a stationary 1.1 MA plasma with ℓ_i=1.07, β_N=4 and $H_{98(y,2)}$=1.1 using a combination of central ECCD (9 MW), mixed on/off-axis NBCD (20 MW total) and 50% bootstrap current. The ideal n=1 stability limit for this case is β_N=4.1 without a conducting wall and β_N=4.8 with a wall. This simulated high ℓ_i case is consistent with the planned upgrades to the DIII-D heating systems.

This work was supported in part by the US Department of Energy under DE-FC02-04ER54609, DE-FG02-04ER54761, DE-AC52-07NA27344, and DE-FG02-08ER54984.

[1] Turco F. *et al* 2015 *Phys. Plasmas* **22** 056113.
[2] Petty C.C. *et al* 2009 *Phys. Rev. Lett.* **102** 045005.
[3] Ferron J.R. *et al*, accepted for publication in *Nucl. Fusion*.
[4] Ferron J.R. *et al* 2005 *Phys. Plasmas* **12** 056126.
[5] Staebler G.M., Kinsey J.E., Waltz R.E. 2007 *Phys. Plasmas* **14** 055909.